




Static and Dynamic Testing of a Road Arch Bridge in Rabka Zdroj, Poland

Paweł Hawryszków¹  and Wojciech Zielichowski-Haber²

¹ Faculty of Civil Engineering, Department of Bridges and Railways,
Wrocław University of Science and Technology,
27 Wybrzeże Wyspiańskiego St., 50-370 Wrocław, Poland
pawel.hawryszkow@pwr.edu.pl

² PlanBis Bridge Engineer, Finsbury St., York, UK

Abstract. Numerical and experimental load test results of the road arch bridge located in Rabka Zdroj town in Poland will be presented in this paper. The bridge under consideration is designed as a reinforced concrete open-spandrel deck arch structure, of a 40 m long effective span between its springing lines, having both arches fixed in abutments. The whole bridge comprises two parallel arch superstructures, which are tied together by a top slab and joint abutments but having separate sets of vertical wide column systems. The structure was analysed using three numerical distinctive FE models, of different levels of details in order to properly assess the sensitivity of numerical results and accurately determine its realistic structural behaviour. The scope of further investigation to validate its structural behaviour included both static (2 cases) and dynamic (6 cases) proof-load testing undertaken on site. As the result, the bridge is considered to be a very interesting research case as it was identified during the site testing, specifically in terms of its intriguing structural behaviour due to thermal effects. The developed numerical models were used for further static and dynamic simulation. In the paper, the results of both numerical analysis and site proof-load testing are thoroughly reported and concluded.

Keywords: Arch road bridge · Proof-load tests · Dynamic testing

1 Introduction

The subject of this research paper is a road bridge over the ravine in Rabka Zdrój, in Poland. The scope of the paper covers the static and dynamic load proof testing [1, 2] of the arch bridge. The main objective of these investigation works undertaken on-site was to assess the structural integrity and overall performance of the arch superstructure against its design assumptions and to verify the agreement of the test results against the requirements detailed in the proof load test design report.

2 General Description of the Structure

The structure under consideration was designed as a single-span, open-spandrel deck-stiffened road arch bridge (Fig. 1), with a clear span of 40.0 m between its springing points. The overall width of its deck is 14.24 m, whereas the width of the double carriageway situated on the deck slab is 12.0 m. The width of both pavements is 2×2.0 m. The skew angle of the bridge and the angle between the bridge central line and the ravine are 90.00° .

The superstructure of the bridge was designed in the form of a single-span, 1.0 m deep reinforced concrete arch girders, thickened in their keys over the length of 12.20 m and fixed to two reinforced concrete abutments. The load-bearing arch consists of two separate, 2.5 m wide arch girders, parallel to each other in a plan and braced with a deck slab by the means of a set of separated solid vertical columns. The bridge deck was designed in the form of a 0.20–0.35 m thick reinforced concrete slab of 13.54 m width and 53.0 m long effective span between the bearing lines of end abutment walls. The deck slab is supported on end abutments by the means of 4 no. bearings at each end and in addition fixed to intermediate vertical columns. The central part of the deck slab is connected monolithically with both arch girders in their keys. Other connections between the arch girders and the deck slab are achieved by the system of cast in situ reinforced concrete columns which provide a type of rigid joints between these elements. These solid vertical columns which connect the deck slab with the arch girders are arranged in 4.0 m spacings along with the bridge span, except for end columns which are located at the distance of 4.5 m from the abutments. As the result, the bridge deck slab along the bridge span is supported on 8 no. vertical solid columns, 6 no. sitting on top face of the arch girders, which transfer all loading from the deck slab down onto the arch girders. The end solid columns are directly tied to concrete foundation slabs, which also support abutment walls.

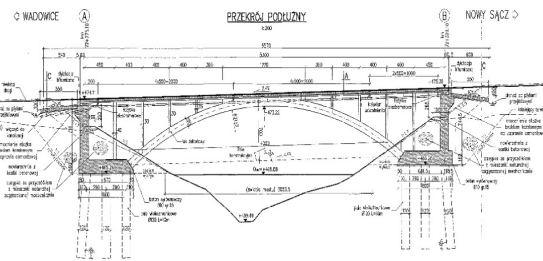


Fig. 1. Arch bridge under consideration and side view of the structure.

3 Analysis Models

Robot Structural Analysis software was used for the modelling and simulating the structural behaviour of the bridge subject to proof test load. Three independent FE models were developed for this purpose: (e^1, d^2) – a plane 2D frame model, in which line beam elements were used to represent columns, arch girders and the deck slab, $(e^1 + e^2, d^3)$ – a spatial 3D beam-shell model, in which arches and columns were defined as beam elements, whereas surface shell finite elements were used to model the deck slab, $(e^2 + e^3, d^3)$ – a spatial 3D shell-solid model, in which surface shell finite elements were used to model the deck slab and columns, solid volumetric finite elements were used to model the arch girders.

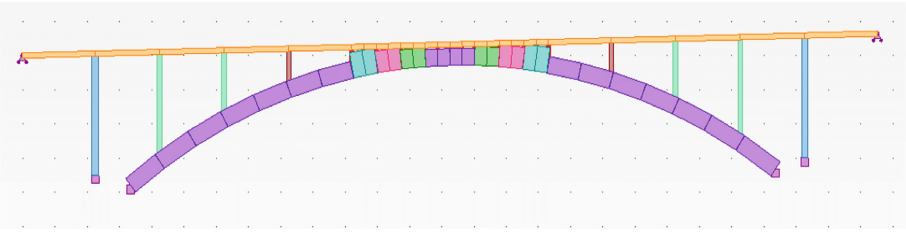
The models were used to determine the value of internal forces and verification of calculations. The spatial beam-shell model was specifically used to determine internal forces in superstructure members and determine their displacements due to the code-based and proof test loading, while the shell-solid model was used to determine the expected deformation of the arch girders caused by the proof test loadings. The plane frame model, serving as an auxiliary model, was used for a generation of influence lines in order to determine the most onerous proof test load positions and subsequently work out the extreme values of internal forces to validate the bridge design to the design standards and the proof test load effects.

The plane frame model as shown in Fig. 2a was developed with the use of line beam elements, to which appropriate geometric properties of the arch girders, deck slab and its supporting columns were consequently assigned. The perfectly rigid links were used in order to accurately model the interface action between the deck slab and the arch girders in the arch key areas. This model does not include the transverse action of two arch girders.

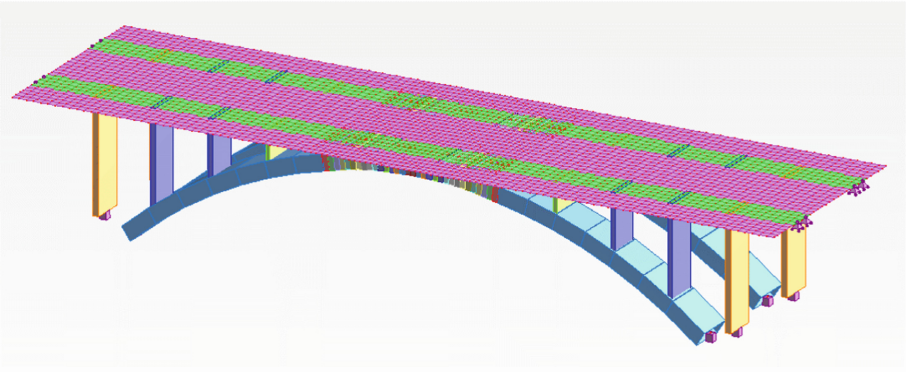
To allow for the realistic, transverse distribution of the applied loads, the spatial FE-based model was developed as shown in Fig. 2b. This model was created with the use of line beam elements to which the arch girders and vertical columns properties were assigned. The deck slab was modelled with the use of surface finite elements of appropriate thickness in order to reflect the actual dimensions of the deck slab and furthermore, to apply the code-based and proof test loads on the deck slab with a greater precision. The connections between the deck slab and the arch girders in their key areas were modelled in an identical way as in the case of the plane frame model with the use of perfectly rigid links.

The third shell-solid FE-based model was developed as shown in Fig. 2c in order to reflect the geometry of the arch girders in the most accurate way, hence to simulate the deformations and the state of stress and strain with a greater precision. The arch girders together with the thickened part at their key section were modelled with volumetric solid elements to represent the real geometry of the arch girders, while the deck slab together with the supporting columns were modelled with shell elements to which the designed thickness was assigned. All spatial models enabled to consider the transverse interaction of two arch girders.

a.



b.



c.

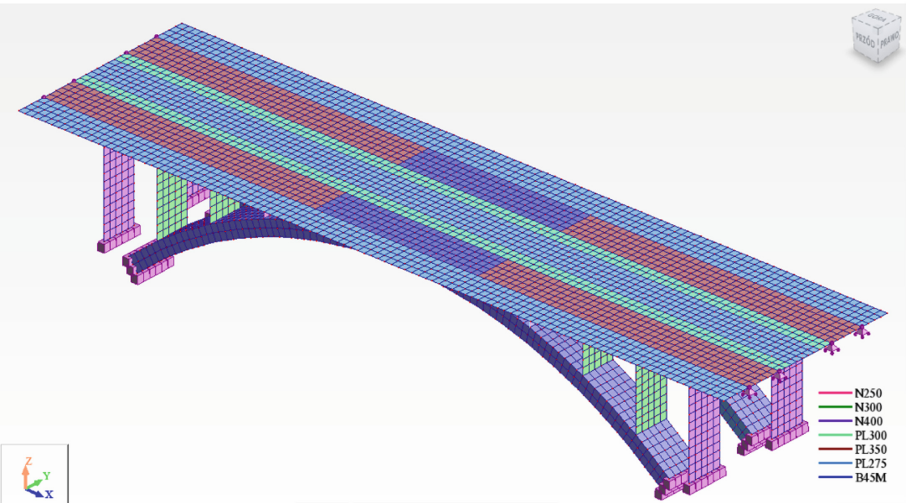


Fig. 2. Bridge models used in FE analyses: a. frame model (e^1 , d^2), b. beam-shell model ($e^1 + e^2$, d^3), c. shell-solid model ($e^2 + e^3$, d^3).

Designed boundary conditions were assigned to all models of the bridge, which was achieved with the use of rigid supports to model fixing connection details between the foundations and arch girders and end vertical columns. On the contrary, the deck slab end edges were supported on the abutment walls using the free supports restrained only in the vertical direction which represented free sliding articulation.

A general view of the superstructure geometries for three computational models developed with the use of FE-based calculation package is presented in Fig. 2.

4 Measurement Equipment

During the static tests, vertical displacements of the arch girders in the longitudinal and transverse direction were measured at the locations of approx. $\frac{1}{4}$, $\frac{1}{2}$ and $\frac{3}{4}$ along the span length. Additional measurements of vertical displacements of the arch girders at their springing points, at their interfaces with foundations on both abutments were carried out with the use of a precise digital level station facilitating the automatic recording of results (measuring accuracy 0.01 mm, refer to Fig. 3).



Fig. 3. Digital level station with the automatic recording of results and surveying of vertical displacements of the arch girders at their springing points and interfaces with the foundations.

During the dynamic tests, the vibrations of the bridge were measured using a laser station from the Finnish company NOPTTEL OY. The principle of the measurement was based on the determining of movements of the photosensitive receiver in relation to a stationary laser beam, which was sent by a transmitter located outside the load impact area. The measurement of vibration displacements with a laser device was used to determine the dynamic overload factor. The B12/200 acceleration sensor having a measurement accuracy of 0.01 m/s^2 was installed at the location of the laser device receiver and subsequently used to determine the frequency of deck slab vibrations. The measuring devices used during this dynamic testing are shown in Fig. 4.



Fig. 4. The laser equipment and acceleration sensors used for dynamic testing.

5 The Scope of Testing

Two static proof load test schemes were performed on site. The testing of the structural performance of both arch girders supporting the deck slab was carried out during the implementation phases for the schemes S-I (Fig. 5) and S-II (Fig. 6). Four trucks with the total weight of 38 tons were used. Regular readings from the measuring devices were performed following the setting up each two vehicles. The purpose of this load staging, in accordance with the schemes shown on the diagrams (A ÷ D), was to assess the span performance at various load phases, finally including the design load.

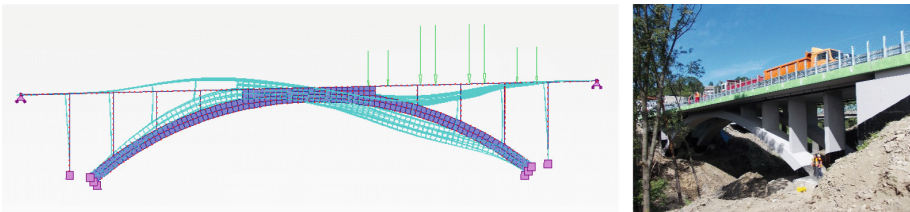


Fig. 5. Testing of the bridge at full proof test load for the scheme S-I.

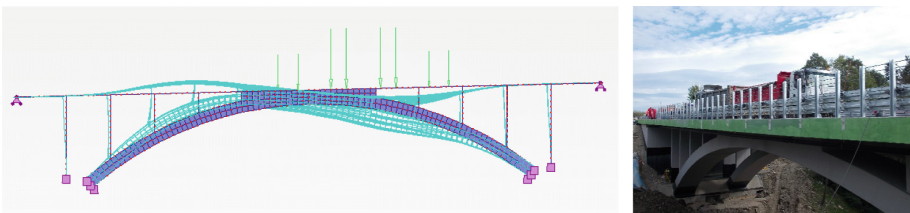


Fig. 6. Testing of the bridge at full proof test load for the scheme S-II.

Dynamic load testing was carried out after the static testing with the use of 1 no. truck vehicle (Fig. 7). Six various scenarios of dynamic excitations were implemented on-site, including 3 no. crossings of the heavy truck moving on a smooth surface of the carriageway and 3 no. crossings of the heavy truck over an artificial road bump at the varied speeds of 10, 30, 50 km/h.



Fig. 7. Passage of the truck on a smooth roadway and through artificial unevenness of the surfacing reflected by a road bump.

6 Numerical and Experimental Results

In the static part of the in-situ testing, the vertical displacements were measured at 10 points. The objective of the static testing was to determine the greatest values of arch girder deflections for both the S-I and S-II testing schemes. The elastic displacements were calculated as the difference between the total value of measured permanent displacement, defined as the final displacement after the loading trucks came off the bridge and the displacement resulting from the settlement of the foundations.

Scheme S-I

The value of permanent vertical displacement at the measurement point no. 04 was $w_{\text{perm}} = 0.00$ mm. The value of the measured, maximal elastic displacement (at the point no. 04) was $w_{\text{ela}} = 2.66 - 0.00 - 0.41 = 2.25$ mm which has not exceed the calculated value from FE-based model $w_{\text{cal}} = 2.41$ mm.

Scheme S-II

The value of permanent vertical displacement at the measurement point no. 09 was $w_{\text{perm}} = 0.02$ mm. The value of the measured, maximal elastic displacement (at the point no. 09) was $w_{\text{ela}} = 2.11 - 0.02 - 0.02 = 2.07$ mm, which matches the calculated value from FE-based model $w_{\text{cal}} = 2.07$ mm.

The example diagram of the deflection at the mid-span cross-section for the scheme S-II is shown in Fig. 8. The surveyed soffit profile indicated a greater rotation of the superstructure subject to the asymmetric proof load on site when compared against the numerical results (this applies to both completed schemes).

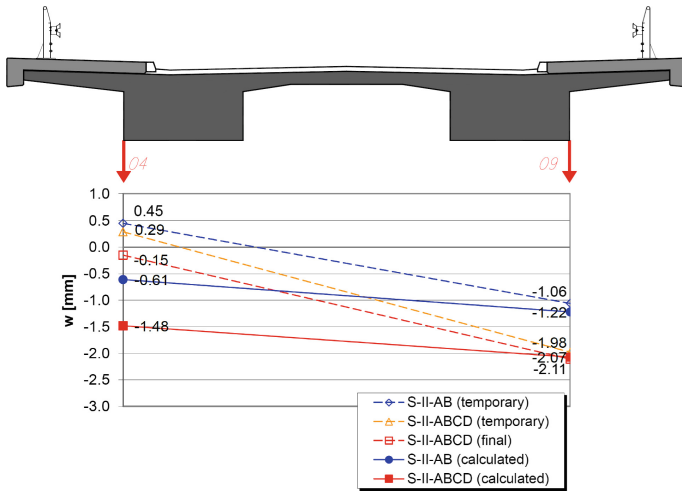


Fig. 8. The deflection profile across the superstructure cross-section for the scheme S-II (calculated values against surveyed values).

The modal shapes of natural vibrations of the superstructure and the corresponding frequencies were determined from the numerical analysis with the use of the FE-based model (see Fig. 9) and were confirmed by testing results (see Table 1).

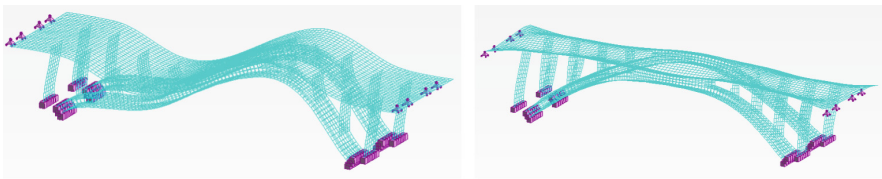


Fig. 9. First and second mode shape for the first natural vibrations (respectively: $f = 4.32$ Hz and $f = 5.53$ Hz).

The natural frequencies of bridge vibrations were identified from the on-site dynamic testing and are presented in the Table 1. The frequencies were determined from the FFT analysis of vibration signal output recorded by the acceleration sensors. The identified natural frequencies are close to the calculated values from the FE analysis.

Table 1. Frequencies of the deck vibrations identified from the test results.

Frequency	Calculations	Scheme					
		S-1-10	S-1-30	S-1-50	B-1-10	B-1-30	B-1-50
f_1 [Hz]	4.32	4.66	4.80	4.56	4.63	4.40	4.80
f_2 [Hz]	5.53	5.14	5.27	5.04	5.07	5.03	–

7 Summary

The static and dynamic tests were performed as a part of the load proof testing procedure for the bridge. The measurement results obtained from the on-site testing proved sufficient structural integrity and robustness of the bridge in relation to its structural and dynamic performance during the testing. However, some significant thermal load effects occurring in its superstructure caused by temperature change were identified as the result of the undertaken numerical analysis. This was largely due to the over constraining effect of the stiff vertical columns which ties the arch girders with the deck slab and in particular, over stiffened monolithic connection at the arches key. The influence of temperature change on load effects in the arch superstructure was found disproportionately high, especially when comparing against the traffic live load effects. Therefore, a further study is undertaken as a continuation of the presented research works which concerns the methods of relieving these effects through appropriate design changes.

References

1. Fryba, L., Pirner, M.: Load tests and modal analysis of bridges. *Eng. Struct.* **23**, 102–109 (2001)
2. Gentile, C.: Modal and structural identification of a R.C. arch bridge. *Struct. Eng. Mech.* **22** (1), 53–70 (2006)